NANO LETTERS

2007
Vol. 7, No. 5
1232−1239

Inner-Tube Chirality Determination for Double-Walled Carbon Nanotubes by Scanning Tunneling Microscopy

Cristina E. Giusca, Yann Tison, Vlad Stolojan, Ewa Borowiak-Palen,† and S. Ravi P. Silva*

Nano-Electronics Centre, Advanced Technology Institute, School of Electronics and Physical Sciences, University of Surrey, Guildford, Surrey GU2 7XH, United Kingdom

Received January 11, 2007; Revised Manuscript Received March 13, 2007

ABSTRACT

Evidence for modified electronic structure in double-walled carbon nanotubes with respect to their individual inner and outer constituent single-walled nanotubes is provided by scanning tunneling microscopy and spectroscopy experiments. The contribution originating from the inner tube to the local density of states of the double-walled system was identified in agreement with previous theoretical calculations. Consequently, the chiral index for the inner tube was extracted based on the additional van Hove singularities present in the experimental tunneling spectra.

While studies of single-walled carbon nanotubes (SWNTs) and also multiwalled carbon nanotubes (MWNTs) are being carried out by different groups, for a full elucidation of the electronic properties of these systems, it is necessary to investigate the electronic and structural properties as a function of the constituent individual graphene walls. This is in order to examine the electronic transitions that occur in the density of states (DOS) when moving from an ideal one-dimensional quantum wire to a more diffused electronic system. The electronic properties of SWNTs are better understood than those of MWNTs, and they are also easier to theoretically simulate and understand using modern high-performance computing.

Some experiments carried out on MWNTs show evidence that, for low bias, transport in these systems is predominantly governed by the outermost shell, while for high bias, the current is carried by a combination of outer and inner shells.[1,2] Other experimental results indicate the presence of ballistic transport in individual MWNTs.[3] The conductance due to intertube transfer was measured in telescopic MWNTs and monitored using a system of nanomanipulator piezo drives within a transmission electron microscope (TEM).[4] These results showed that the resistance between the ends of a multiwall carbon nanotube during telescopic extension of the nanotube increases monotonically with extension, demonstrating that a telescoping nanotube constitutes a near-ideal nanometer-scale rheostat. Theoretical calculations on the transport properties in MWNTs show a small intertube transfer component owing to the difference between the crystal momentum or k vector of the inner and outer shells.[5]

However, it is still unclear as to whether there is a definite relationship between the intershell coupling, the helicity of the constituent tubes, and the electronic properties of these systems. In this respect, double-walled carbon nanotubes (DWNTs) are the easiest system to work with, both experimentally and theoretically, as it only contains two constituent shells, and based on the interaction observed, conclusions can be more accurately drawn as to the cause of the observed results. A system containing only two layers should be simpler to model theoretically than a multilayer system, as it can be obtained by adding an outer layer to a SWNT, and therefore correlations between the two layers can be studied in more detail and subsequently applied to systems containing multiple layers.

Recently, Raman spectroscopy[6,7] or electron diffraction experiments were performed on DWNTs by various groups. Nanoarea electron diffraction (NAED) experiments showed that it is possible to determine the chiralities and reconstruct the image of a DWNT from the diffraction patterns of the tube with a resolution of 1 Å,[8] whereas Raman spectroscopy provided evidence for atomic correlation and electronic structure change of the two constituent tubes in DWNTs.[7] The electronic structure of DWNTs was also probed by Kociak et al.,[9] by in situ transport measurements in a TEM on individual DWNTs simultaneously with the use of selected area electron diffraction (SAED) to assign the chiralities of constituent tubes. Despite the great success of

* Corresponding author. E-mail: s.silva@surrey.ac.uk.
† New address: Department of Hydrogen Technologies and Nanomaterials, Institute of Chemical and Environment Engineering, Szczecin University of Technology, Pulaskiego Street 10, 70-322 Szczecin, Poland.

10.1021/nl070072p CCC: $37.00
Published on Web 04/14/2007

scanning tunneling microscopy (STM) in probing both the structure and the electronic properties of SWNTs, there are no reported STM and scanning tunneling spectroscopy (STS) studies linking the chiral indices of the inner shells to the electronic properties of the MWNTs. This is because the STM will only resolve the chirality of the outermost shell. We have performed UHV-STM experiments on DWNTs in an attempt to investigate whether the overall electronic structure is dependent on the interaction between the inner and outer layers or it is only a function of the outer layer chirality pair, as was previously suggested.[10] The normalized tunneling conductance ($V/I(\mathrm{d}I/\mathrm{d}V)$) as measured in our STM and STS experiments gives us direct access to the electronic level structure of the nanotube (the local DOS),[11] thus providing a measure of interacting potentials for modifications of the local DOS. We show in this paper that it is possible to identify the contribution of the inner tube in a DWNT and extract its chirality based on the van Hove singularities present in the DOS spectra revealed by STS.

Pure tubes, free from amorphous carbon coatings, are crucial for STM experiments in order to obtain the atomic resolution required for a complete characterization of the tubes. Therefore, we have used the following procedure to purify the nanotube material. The DWNTs used in this work have been purchased from Carbon Nanotechnologies, Inc. and were first refluxed for 40 h in 2 M HNO_3 at 150 °C, then washed with deionized water and filtered using a microsyringe and Whatman filter. After drying, the tubes were refluxed again for 45 min using 2 M HCl at 150 °C. The reflux was followed by a large number of washing cycles with deionized water, after which it was filtered and allowed to dry. As a final step, the resulting material was oxidized in air for 1 h at 300 °C. After the purification procedure, the mass of the product was found to decrease to approximately half the value of the initial mass. The weight loss is mainly attributed to the removal of the catalyst particles from the raw sample, as a result of the acid refluxing, which is also known to open the caps of the nanotubes.

For STM experiments, a suspension of DWNTs was prepared by sonication in 1,2- dicholoroethane for approximately 15 min and then drop-cast on atomically flat Au substrates prepared following a method described in ref 12. The sample was left in the fast entry lock of the system prior to introducing it into the STM chamber and pumped overnight to allow for the specimen to outgas. The base pressure in the STM chamber did not exceed $(2-3) \times 10^{-11}$ mbar during the entire set of STM experiments. Typical scanning conditions used with this sample were 0.1 nA for the tunneling current and a positive (unless otherwise specified) bias for the sample of (0.1−0.3) V. The STS measurements were performed by interrupting the scanning and the feedback at preset locations and recording the current variations during the voltage ramp (usually between −3 and +3 V).

TEM was used to assess the quality of the samples. Specimens for TEM were prepared on holey C grids after dispersing the purified material in ethanol (99.99% purity) using an ultrasonic bath. The suspension was drop-cast on the grid and allowed to dry in air, after which a 200 kV Philips CM200 TEM (LaB_6 source) fitted with a Gatan imaging filter (GIF2000) was used to investigate the DWNT sample. The current density was ∼75 A/cm^2, and the microscope was calibrated immediately prior to the irradiation experiment. Changes in the microscope lenses were kept to a minimum when switching to the nanotubes. Calibration was checked against the graphite 002, resulting in a measurement error of ± 0.05 Å. More details of the sample preparation can be found in the Experimental Details section which follows. Some representative samples suitably prepared are shown in Figure 1.

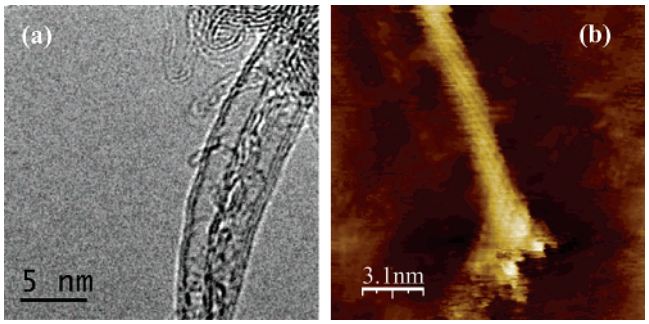

Figure 1. (a) TEM image of double- and triple-walled carbon nanotubes and (b) STM image of an isolated nanotube showing an opened end covered by amorphous carbon, as a result of acid refluxing.

Both inner and outer diameters for the two constituent tubes of DWNTs were estimated from TEM images, and it was found that the inner diameters vary from 0.9 to 1.9 nm, whereas the outer ones from 1.9 to 2.6 nm, with a wall spacing ranging from 0.30 to 0.54 nm.

However detailed the information obtained by TEM, the chiral indices (n,m) that determine whether a SWNT will be a metal or a semiconductor are not accessible from these images, as made possible by STM, which allows for a direct chirality identification.

The STM images generally revealed bundles of DWNTs and occasionally individual tubes. Atomic resolution was obtained on some of the investigated DWNTs, as illustrated in Figure 2, which also shows its fast Fourier transform (FFT) image, together with a zoomed image on the central part of the tube, showing the C honeycomb lattice. The images in Figure 2 show the typical lattice of C hexagons, with the dark areas being the center of the hexagons. The distance between the neighboring centers of the hexagons is ∼0.25 ± 0.01 nm, comparing well with the known value for graphite. The hexagons appear slightly distorted at some locations (more visible in Figure 2c). It is unlikely that these distortions are due to thermal drift, as thermal drift would affect the whole image, and images recorded successively before and after the one shown in Figure 2a do not display any noticeable drift from one frame to the other. Van der Waals interactions between the tubes in a bundle could be responsible for inducing a certain degree of stress because of the tubes being packed within the bundle with the condition of minimizing the conformational energy. As a

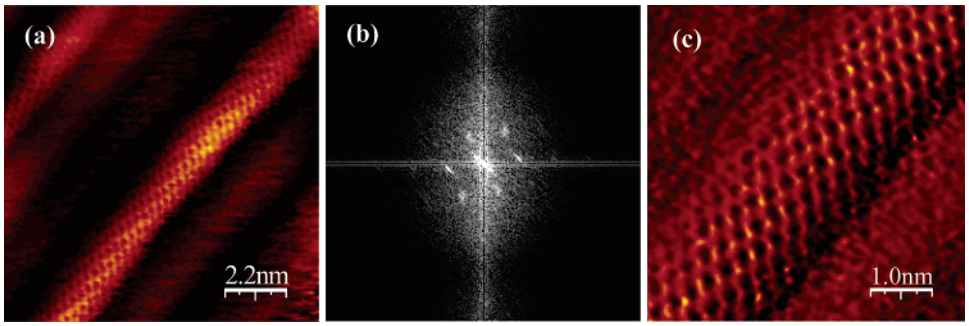

Figure 2. (a) STM image showing atomic resolution of a DWNT on top of a bundle, (b) FFT taken on a rectangular area (8×8 nm^2) on the central part of the DWNT, and (c) derivative image of a zoomed region of the DWNT. The derivative was preferred instead of the raw image, as it shows better, enhanced contrast.

result, some tubes may appear twisted within the bundle, and this could lead to local distortions of these tubes or others located on top or next to them.

By carefully examining the tube in Figure 2a, one can observe that the central region of this tube lies slightly higher topographically than the remainder, probably due to the aspects discussed above or because it is following the contours of substrate features.

Different atomic sites, best visible on the image in Figure 2c, display a difference in contrast, with some atoms appearing brighter than others (which appear darker), reminding one of the nonequivalence between the A-site and B-site atoms observed on graphite, with B atoms visible or brighter than the A atoms in the STM images.[13]

In the case of highly oriented pyrolytic graphite (HOPG), one of the models used to explain this effect is attributed to the asymmetry of the interlayer interactions, which cause an energy dispersion of almost 1 eV along the chains of A atoms normal to the layers. The negligible interlayer interaction along the analogous chains of B atoms yields no such dispersion.[13] The A sites are believed to have lower DOS due to the hybridization with atoms located directly in the layer underneath, and so they are expected to be not visible or less visible than the B sites (with no neighbors in the adjacent layer below) in the STM image. On the basis of the similarity with graphite and as previously observed on MWNTs,[13] the fact that not all C sites on the tube display the difference in brightness could be a consequence of the interwall interaction, suggesting also different chiralities for the two constituent shells of the DWNT and indicating the atoms in the outer shell with or without a corresponding atom of the inner shell located directly underneath.

The resolved atomic structure of this nanotube allows for its chirality determination. To determine the chirality of a nanotube, both the diameter and the chiral angle are needed.[14−16] Careful consideration must be ensured for an accurate evaluation of their chirality, as the size and shape of the tip, as well as the circular shape of the tube combined with the tendency of the tunneling current to follow the shortest path, can induce distortions in the STM image of the nanotube lattice. The result is an apparent broadening of the nanotube with a stretched atomic lattice in the direction perpendicular to the tube.[17,18] No apparent distortion was observed on the lattice of the nanotube in Figure 2, as the angle between the armchair and zigzag directions measured on various sites on the nanotube does not deviate from 30°. Following the method of Odom et al.[19] of determining the chiral angle as the angle of the tube axis relative to the zigzag direction for chiral angles $<15°$, and relative to the armchair direction for chiral angles $>15°$, we obtain a value $(21 \pm 0.5)°$. The same value is obtained by determining the chiral angle using the FFT of the atomically resolved image (Figure 2b) by measuring the angle between the lattice vectors and the tube axis.

For an accurate diameter determination, a simple phenomenological tunneling model for deconvoluting the tip contribution to the image was proposed by Kim et al.[20] by considering the existence of two tunneling gaps, one between the tip and the nanotube and the second between the nanotube and the Au surface. However, for the present case, as the investigated nanotube is not located directly on the substrate, it is difficult to estimate the number of nanotubes between the tube and the substrate, and this may lead to errors due to the unknown tunneling distances. As the apparent height profile is highly dependent on the imaging conditions (bias voltage, etc.) and on the adsorption distance of the nanotube above the substrate, we prefer extracting the diameter from the width of the profile, which might not seem very robust, as it is subject to geometrical convolution with the tip.

A value of 1.98 nm was found for the nanotube diameter as derived from averaging 10 cross-sectional profiles taken across the tube based on the STM image. This value is in very good agreement with the diameter obtained from the separation between the band edges in the experimental DOS of the outer shell of the nanotube (Figure 3). The separation is given by theory for semiconducting nanotubes[21] as: $E_g = 2\gamma_0 a_{CC}/d$, where E_g represents the energy gap (which we determined from the experimental tunneling spectra to be $\sim$0.43 eV), γ_0 the nearest-neighbor overlap integral (taken as 2.9 eV[17]), a_{CC} the distance between two neighboring C atoms (0.142 nm), and d the diameter of the nanotube.

On the basis of the values so determined for the chiral angle and diameter, the chiral indices (18,10) are determined and are such as for a tube that should portray semiconducing characteristics.

To investigate how the observed structural aspects correlate to the electronic structure, we have performed STS by recording current−voltage curves at preset locations along

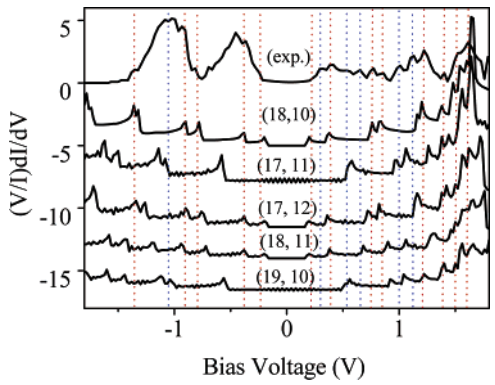

Figure 3. Experimental DOS of the DWNT with a (18,10) chirality for the outer shell (top spectrum) and calculated DOS for (17,11), (17,12), (18,11), and (19,10).[22] DOS spectra are shifted vertically for clarity. Blue dotted lines highlight the peaks in the experimental DOS spectra that could not be assigned to a corresponding peak in the calculated (18,10), while red dotted lines show the peaks that have a correspondent in the calculated (18,10) spectrum.

the tube and on the Au substrate, with the curves recorded on Au appearing linear. Consistent behavior is observed on most STS curves recorded along the tube, similar to the ones shown in the inset in Figure 3. Some of the curves show flat regions on the high negative or high positive bias side, which is due to preamplifier saturation. A number of the 25 curves have been recorded, and the typical normalized differential conductance, which is a measure of the local DOS, was obtained after numerical derivation (Figure 3). The curves show low conductance at low bias and asymmetric peaks as the voltage increases, peaks which correspond to the familiar van Hove singularities (vHs) typical to the one-dimensional systems, at the onsets of the energy bands of the CNT. The obtained normalized differential conductance spectra exhibit no visible shift of the Fermi level as usually reported in the literature due to the interaction with the substrate.

Also included for comparison in Figure 3 are the calculated DOS for the (18,10) and for the next closest chiralities, (17,11), (17,12), (18,11), and (19, 10). The calculations were performed using the density functional theory with local density approximation and made available by Akai and Saito.[22]

Out of all the calculated spectra, it can be seen that the tunneling spectra for (18,10) and (17,11) show the closest resemblance to our experimental DOS, except for some additional peaks, whose origin will be discussed later in the paper. However, after a very careful analysis of many DOS spectra acquired at about 25 different locations on the tube, we conclude that most curves seem to match more closely the (18,10) calculated spectrum rather than the (17,11) spectrum, a fact supported also by the chirality assignment based on the diameter and the chiral angle determined from the atomically resolved structure in the STM image. What must be highlighted is that absolutely all of the investigated normalized differential conductance curves display a nonzero DOS at the Fermi level, which is not consistent with a semiconducting tube as a SWNT with (18,10) chirality would be.

The presence of a nonzero DOS at the Fermi level suggests that the inner tube might have an effect on the electronic properties of the DWNT system, as also evidenced by the observed difference in brightness for some of the constituent C atoms.

A finite density of states within the gap, observed in the normalized conductance spectra for this tube, could also be possibly attributed to effects such as band bending induced by the tip states or residual tunneling coming from the Au substrate through the tube or from other neighboring tubes.

Doping by charge transfer from the substrate is possible considering the difference between the work function of Au and the one of the CNT. This would, however, shift the Fermi energy toward the valence band by $\sim(0.1-0.3)$ eV due to the charge transfer inducing a local electrostatic potential perturbation on the nanotube side, as observed in other STS experiments on individual SWNTs and small ropes.[15,23] Interestingly, large bundles were found not to exhibit a shift. We do not observe a shift of the Fermi level for the investigated nanotube, and the semiconducting gap seems to be symmetrically positioned around the Fermi level, suggesting a negligible contribution from the substrate or a large bundle. A large bundle would be unlikely, as indicated by the line profiles across the tube. However, as evidenced by previous STM studies on carbon nanotubes, the substrate does not perturb the band structure of the nanotube.[23]

It was theoretically predicted[23−25] and experimentally shown[26] that the electronic properties of nanotubes packed within a bundle are affected by nanotube−nanotube interactions. In armchair (n,n) nanotubes, a pseudogap was found to appear due to the broken rotational symmetry of the rope environment, allowing for mixing of symmetric π and antisymmetric π^* states, but the rest of the band structure was left unaltered. It is not clear to what extent the band structure of chiral tubes as the one presented in the current study would be affected by the intertube interactions within a bundle, and this point would need to be examined further by theoretical calculations. However, other tubes in the bundle would be expected to contribute less to the surface DOS of the currently investigated DWNT than the inner tube.

The nanotube under study is part of a bundle, which is in addition possibly lying on a step, and van der Waals interactions between nanotubes and with the substrate can result in radial and axial deformations, which can modify the idealized geometry of free nanotubes.[27,28] However, unless the nanotube undergoes drastic deformations, such as radial collapse, the electronic properties have been shown to appear quite robust under mild deformations.[29,30] Moreover, it should be expected that the electronic properties would be modified in the vicinity of the step but not a few nanometers away from it, and the $I-V$ curves show consistent behavior 5 nm away to the left and right of the step, so the step contribution can be excluded. When nanotubes are part of a bundle, they may appear twisted in an attempt to minimize the conformational energy,[31] and this could also be responsible for modifying the electronic properties. However, it is unlikely that this nanotube is

twisted, as we obtain the correct 30° angle between the armchair and zigzag direction.

On the basis of the aforementioned theoretical and experimental studies, we will assume that even if the substrate and the intertube interactions might have a contribution to the finite density of states we observe at the Fermi energy, the band structure will not be modified.

The observed difference in brightness displayed by some of the constituent C atoms in Figure 2c brings evidence for interaction between the layers of the DWNT, suggesting that the inner tube might have an effect on the electronic properties of the DWNT system and might contribute to the overall DOS. It is worth mentioning that data obtained from SWNTs[15,16,19] present no site-to-site variation, showing the honeycomb structure of all six C atoms, as expected. Although the role of the substrate and of the intertube interactions in the bundle cannot be completely ruled out, a finite density of states at the Fermi energy would be in accordance with other previous studies showing that DWNTs, and more generally MWNTs, exhibit metallic behavior.

To get a better idea about the effect the inner tube might exert on the electronic properties of the whole system, a careful analysis of the tunneling spectra recorded along this tube was performed. A detailed analysis of the experimental tunneling spectra reveals the peaks corresponding to the van Hove singularities of a (18,10) tube, but some extra peaks can be identified, and they are indicated by the blue dotted lines in Figure 3.

The LDA DOS has high accuracy in predicting the relative positions of peaks and peak shapes both for valence-band and the conduction-band region, while the value of the fundamental gap of semiconductors and insulators is known to be underestimated in the LDA.[32,33] This should possibly account for the small deviations observed between the vHs positions between the experimental data and theoretical calculations. However, reasonable agreement is obtained between theory and experiment. As our measurements were carried out at room temperature, meaning an STS resolution of the order of 4 k_BT, which amounts to $\sim$0.1 eV,[34] this allowed us to consider all the peaks spaced larger than 0.1 eV as real features. The broadening of the peaks can be attributed to thermal effects or to hybridization effects between the nanotube molecular orbitals and the Au atomic orbitals as well as curvature-induced hybridization that could give rise to band repulsion.[15,19]

A possible explanation for the existence of these extra peaks could be that they are due to the interlayer interaction between the two constituent tubes or simply due to the inner tube itself in accordance with a theoretical study carried out on DWNTs by Saito et al.,[35] which shows that when the interlayer interaction between the double layers is not considered, the energy dispersion relations are just the overlay of the energy dispersion relations of the unperturbed inner and outer tubes. Their study examined the electronic structure of various combinations of metallic and semiconducting constituent inner and outer layers, associated to different diameter and chirality of the tubes, for commensurate and incommensurate arrangements of the two layers. A DWNT is called commensurate if the ratio between the unit cell lengths along the tube of the two constituent shells is a rational number and incommensurate if this ratio is irrational. For large diameters, as is our case, the two tubes are expected to be incommensurate, and two incommensurate tubes are expected to have only 2π rotational symmetry along the chiral vectors that are both perpendicular to the nanotube axis. Thus, the energy bands of the inner tubule are not degenerate with those of the outer tubule. Therefore, the electronic properties of an incommensurate DWNT can be considered to be the sum of the electronic structures of two independent nanotubes except for some small modifications due to a weak interlayer interaction.[35] On the basis of the existence of the extra peaks observed in the tunneling spectra assigned to the inner tube, the chirality of the inner tube can be estimated. By observing the difference in radii between the inner and outer tubes obtained using the interlayer spacing estimations from the TEM measurements, we can determine the radius of the inner tube. From the TEM measurements, an interlayer spacing between 0.30 and 0.53 nm was obtained, which, subtracted out of the 1.98 nm, which is the diameter of the tube from the STM image, suggests that the inner tube diameter should be in the range 0.92−1.38 nm. In this range of diameters, there are 40 possible chiralities, with 14 metallic and the rest semiconducting tubes. As it was recently shown by HRTEM combined with electron diffraction (ED) experiments on DWNTs, no correlation in the chiral angle between the inner and outer tubes exists.[36] Therefore, there is no way to eliminate some of the chiralities based on structural considerations. Reducing the number of possible chiralities can be done by taking into account electronic effects. Because the outer layer, as determined by the chiral coefficients of our STM image, is semiconducting and based on the theoretical work of Saito et al.[35] that semiconducting−semiconducting tubes do not become metallic by introducing an interlayer interaction, two semiconducting tubes cannot account for the nonzero DOS at the Fermi energy that we observe for the present DWNT. Thus, having the outer layer of our DWNT semiconducting, an interlayer interaction evidenced by the difference in brightness of C atoms, and a finite DOS at the Fermi level, the featured DWNT can only contain a metallic inner tube, which reduces the number of possible chiralities for the inner tube to 14. Table 1 presents the possible chiral indices in the above-stated range of interest for the inner diameter.

For the case of DWNTs containing a semiconducting outer and a metallic inner tube, the detailed energy dispersion relations seem to be affected by the interlayer interaction, showing anticrossing of energy bands and splitting of the energy bands for the inner and outer tubes.[35] But, the combination inner−outer tube retains the basic electronic properties of each constituent.

On the basis of the above considerations, we can thus use the calculated DOS for the tubes listed in Table 1 and compare it to our experimental tunneling spectra to identify the ones whose singularities would account for the observed extra peaks. After careful comparison with the calculated DOS, we believe that the chirality pairs (11,5) and (12,3)

Table 1. Possible Chiral Indices (*n*,*m*) of Metallic Nanotubes Having the Diameter between 0.9 and 1.30 nm

n	*m*	diameter (nm)	chiral angle (deg)
7	7	0.96	30
8	8	1.1	30
9	6	1.03	23.4
9	9	1.23	30
10	4	0.99	16.1
10	7	1.17	24.1
11	2	0.96	8.2
11	5	1.12	17.8
12	3	1.09	10.9
12	6	1.26	19.1
13	1	1.07	3.7
13	4	1.22	13
14	2	1.20	6.6
15	0	1.19	0

provide the best match to our experimental data, as the constituent peaks of these spectra could account for most of the extra peaks observed in the STS spectra on our DWNT. Figure 4 shows the calculated and the experimental tunneling spectra for the (18,10) chirality corresponding to the outer tube, together with the calculated spectra for (11,5) and (12,3), indicating the peaks assumed to belong to the inner tube by dotted lines.

The agreement seems to be better above the Fermi level, which contrasts with earlier STS measurements on SWNTs, which have reported larger deviations from the calculated DOS of SWNTs for the conduction band.[20,37] This was attributed to curvature-induced hybridization effects being much higher for π^*/σ^* orbitals than for π/σ, affecting more the bands above the Fermi energy, as shown by ab initio calculations.[38] In our case, however, it seems that a more pronounced inconsistency is observed for the filled rather than for the empty states with respect to the calculated DOS. Apart from the peak at ~ -0.4 eV, which could be attributed to the Au surface state,[39] the other contributions could possibly come from the interaction between the layers.[35]

The diameters and chiral angles necessary to obtain the above specified chiral pairs are 1.09 nm and 11° for (12,3) and 1.13 nm and 18° for (11,5), and they correspond to an interlayer spacing of 0.45 nm for (12,3) and 0.43 nm for (11,5), respectively.

If we consider the exponential decay of the tunneling current with the distance, one would intuitively expect the contribution of the inner layer to be a few orders of magnitude smaller than the one of the outer layer. However, it was shown for the case of C60 molecules inside SWNTs that the characteristic feature of peapods appears in the STM images showing both atomic corrugation of the SWNT and features associated with the encapsulated C60 molecules.[40]

Regardless of which one of the two possible chiralities for the inner tube is considered, this DWNT is of incommensurate type, as the calculated ratios of the unit cell length for the outer to inner tube are irrational.

The incommensurate DWNTs are similar to turbostratic graphite, meaning that the neighboring layers are not stacked

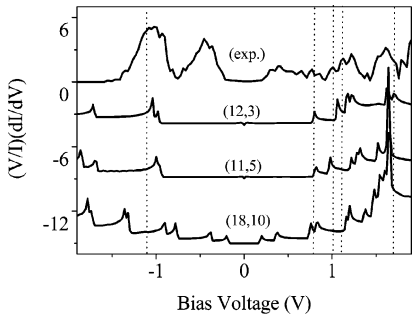

Figure 4. Experimental and calculated DOS for (18,10) corresponding to the outer tube and calculated DOS[22] for two possible chiralities for the inner tube, (12,3) and (11,5).

with respect to one another with good atomic correlation.[7] Therefore, the interlayer interaction between the neighboring layers is weakened in comparison to 3D graphite. A weak interlayer interaction for our DWNT is supported by the fact that the spacing between the two constituent shells is greater than the typical known interlayer distance in graphite (0.34 nm). Also, the observed van Hove singularities of the DWNT do not seem to be modified with respect to those of the constituent tubes, consistent again with a weak interaction between the two walls, interactions which could, however, induce the presence of some additional peaks as predicted by theory.

Some of the peaks in the experimental spectra are still not accounted for when considering the van Hove contributions of the inner tube, and their origin is still to be understood. A defect on the inner tube might be a possible explanation for their presence, but as the $I(V)$ curves were taken at many locations along the tube and most of them show consistent behavior, we can therefore exclude the explanation based on a defect. Another explanation might be that they originate from the formation of an interlayer state in the region between the walls, as was evidenced for some particular configurations of DWNT.[41] This interlayer state accommodates the extra charge that is found in the region between the two tubes due to π electron depletion on either the outer or inner walls. The charge transfer is found to occur from the inner to the outer tube, as well as from the outer to the inner tube, and seems to follow no pattern based on the tubes' diameter or chirality.

The same treatment as above can apply to other tubes in the same sample that were found to display a semiconducting outer layer and a finite DOS at the Fermi energy, although more experimental work is needed on individual isolated DWNTs, seconded by theoretical modeling, to enable a firm conclusion on the electronic effects in these systems.

Unlike some earlier transport experiments indicating that it is the outermost shell that dictates the conduction in MWNTs, we present the case of DWNTs that despite having a semiconducting outer layer show finite DOS at the Fermi level. We attribute this to the contribution that the inner tube has to the overall DOS of the DWNT system and, although some existing theoretical models can explain this behavior, further calculations on the specific case presented in this paper are needed to completely understand the interactions.

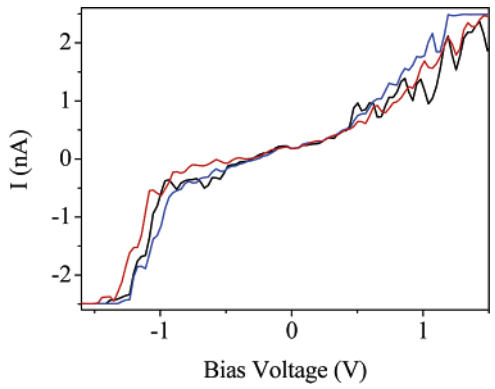

Figure 5. *I*−*V* curves recorded by STS at points along the tube.

The additional van Hove singularities in the experimental tunneling spectra of DWNTs bring evidence for a modified electronic structure compared to the individual constituent SWNTs and provide the source for inferring the chirality of the inner tube. Our results indicate the potential for tuning the electronic properties in a predictable manner for electronic applications.

Experimental Details. SWNTs, as well as some tubes containing three or four layers were occasionally found by TEM in the purified material, which was observed to contain mostly DWNTs (>95%), and in some cases, amorphous carbon and catalyst particles. The amorphous carbon was probably not always effectively removed, given the low oxidizing temperature (300 °C) used for the final purification step. Higher temperatures, usually exceeding 350 °C, although more effective in burning the amorphous carbon, can partially or totally destroy the nanotubes, subject to the nature and purity of the CNTs and to the presence of defects on the tubes. As shown by TEM images (one of which is presented in Figure 1a), the DWNTs occurred as bundles of two−three to tens of nanotubes, as well as larger bundles, and more rarely as individual DWNTs, owing to the purification process which, by removing some of the amorphous carbon, allows the tubes to effectively stick together in bundles due to the increased surface energy. TEM also showed evidence of opened end tubes, most of the time showing C fragments at the end and an asymmetrical shape at the tip. The asymmetrical shape of the opened ends of the purified DWNTs was also evidenced by the STM measurements (Figure 1b).

The instrument used for the STM studies is a commercial Omicron STM/SEM HC, combining STM with scanning electron microscopy. Prior to STM experiments, scanner calibration was carried out on highly oriented pyrolitic graphite (HOPG), which also helped with assessing the quality of the tip by rendering the atomic resolution. STM tips were electrochemically etched W wire prepared immediately before introducing them into the UHV chamber, and their cleanliness as well as the proper calibration of the scanner was checked against the atomic steps encountered on the Au substrate. *I*−*V* curves recorded on clean regions of Au displaying metallic behavior also bring confirmation of a suitable clean STM tip. All measurements were carried out at room temperature in constant current mode. STS was performed at selected locations on the sample by interrupting the feedback for 40 μs, during which an $I(V)$ curve was taken with a preset number of points (usually 300 points), for the bias voltage scan (usually between −3 and +3 V). While the feedback loop was off, the lateral scanning was also interrupted and the tip kept at a fixed distance from the sample. Some of the *I*−*V* curves so obtained are presented in Figure 5. STM images were processed using the WSxM free software available for download at http://www.nanotec.es.

Acknowledgment. We acknowledge financial support from the EPSRC in the form of a Portfolio Partnership award and Dr Y. Hayashi for providing the DWNTs.

References

(1) Bachtold, C.; Strunk, J. P.; Salvetat, J. M.; Bonard, J. M.; Forro, L.; Nussbaumer, T.; Schonenberger, C. *Nature* **1999**, *397*, 673.
(2) Collins, P. G.; Hersam, M.; Arnold, M.; Martel, R.; Avouris, Ph. *Phys. Rev. Lett.* **2001**, *86*, 3128.
(3) Urbina, A.; Echeverria, I.; Perez-Garrido, A.; Diaz-Sanchez, A.; Abellan, J. *Phys. Rev. Lett.* **2003**, *90*, 106603.
(4) Cummings, J.; Zettl, A. *Phys. Rev. Lett.* **2004**, *93*, 086801.
(5) Yoon, Y.-G.; Delaney, P.; Louie, S. G. *Phys. Rev. B* **2002**, *66*, 073407.
(6) Li, F.; Chou, S. G.; Ren, W.; Gardecki, J. A.; Swan, A. K.; Unlu, M. S.; Goldberg, B. B.; Cheng, H.-M.; Dresselhaus, M. S. *J. Mater. Res.* **2003**, *18*, 1251.
(7) Ren, W.; Li, F.; Tan, P.; Cheng, H.-M. *Phys. Rev. B* **2006**, *73*, 115430.
(8) Zuo, J. M.; Vartanyants, I.; Gao, M.; Zhang, R.; Nagahara, L. A. *Science* **2003**, *300*, 1419.
(9) Kociak, M.; Suenaga, K.; Hirahara, K.; Saito, Y.; Nakahira, T.; Iijima, S. *Phys. Rev. Lett.* **2002**, *89*, 155501-1.
(10) Frank, S.; Poncharal, P.; Wang, Z. L.; de Heer, W. A. *Science* **1998**, *280*, 1744.
(11) Stroscio, J. A.; Feenstra, R. M.; Fein, A. P. *Phys. Rev. Lett.* **1986**, *57*, 2579.
(12) Hegner, M.; Wagner, P.; Semenza, G. *Surf. Sci.* **1993**, *291*, 39.
(13) Hassanien, A.; Mrzel, A.; Tokumoto, M.; Tomanek, D. *Appl. Phys. Lett.* **2001**, *79*, 4210.
(14) Dresselhaus, M. S.; Dresselhaus, G.; Avouris, P. *Carbon Nanotubes: Synthesis, Structure, Properties, and Applications*; Springer: Berlin, 2001.
(15) Wildöer, J. W. G.; Venema, L. C.; Rinzler, A. G.; Smalley, R. E.; Dekker, C. *Nature* **1998**, *391*, 59.
(16) Odom, T. W.; Huang, J. L.; Kim, P.; Lieber, C. M. *Nature* **1998**, *391*, 62.
(17) Venema, L. C.; Meunier, V.; Lambin, Ph.; Dekker, C. *Phys. Rev. B* **2000**, *61*, 2991.
(18) Meunier, V.; Lambin, Ph. *Phys. Rev. Lett.* **1998**, *81*, 5588.
(19) Odom, T. W.; Huang, J. L.; Kim, P.; Ouyang, M.; Lieber, C. M. *J. Mater. Res.* **1998**, *13*, 2380.
(20) Kim, P.; Odom, T. W.; Huang, J. L.; Lieber, C. M. *Carbon* **2000**, *38*, 1741.
(21) Dresselhaus, M. S., Dresselhaus, G., Eklund, P. C. *Science of Fullerenes and Nanotubes*; Academic Press: San Diego, CA, 1996.
(22) Akai, Y.; Saito, S. *Physica E* **2005**, *29*, 555.
(23) Odom, T. W.; Huang, J.-L.; Kim, P.; Lieber, C. M. *J. Phys. Chem. B* **2000**, *104*, 2794.
(24) Maarouf, A. A.; Kane, C.; Mele, E. J. *Phys. Rev. B* **2000**, *61*, 11156.
(25) Delaney, P.; Choi, H. J.; Ihm, J.; Louie, S. G.; Cohen, M. L. *Nature* **1998**, *391*, 466.
(26) Ouyang, M.; Huang, J. L.; Cheung, C. L.; Lieber, C. M. *Science* **2001**, *292*, 702.
(27) Hertel, T.; Walkup, R. E.; Avouris, P. *Phys. Rev. B* **1998**, *58*, 13870.
(28) Tersoff, J.; Ruoff, R. S. *Phys. Rev. Lett.* **1994**, *73*, 676.
(29) Lu, J.-Q.; Wu, J.; Duan, W.; Liu, F.; Zhu, B.-F.; Gu, B.-L. *Phys. Rev. Lett.* **2003**, *90*, 156601.
(30) Park, C.-J.; Kim, Y.-H.; Chang, K. J. *Phys. Rev. B* **1999**, *60*, 10656.
(31) Clauss, W.; Bergeron, D. J.; Johnson, A. T. *Phys. Rev. B* **1998**, *58*, R4266.

(32) Miyake, T.; Saito, S. *Phys. Rev. B* **2003**, *68*, 155424.
(33) Miyake, T.; Saito, S. *Phys. Rev. B* **2005**, *72*, 073404.
(34) Wiesendanger, R. *Scanning Probe Microscopy: Methods and Applications*; Cambridge University Press: New York, 1994.
(35) Saito, R.; Dresselhaus, G.; Dresselhaus, M. S. *J. Appl. Phys.* **1993**, *73*, 494.
(36) Hirahara, K.; Kociak, M.; Bandow, S.; Nakahira, T.; Itoh, K.; Saito, Y.; Iijima, S. *Phys. Rev. B* **2006**, *73*, 195420-1.
(37) Márk, G. I.; Biró, L. P.; Gyulai, J. *Phys. Rev. B* **1998**, *58*, 12645.
(38) Kim, P.; Odom, T. W.; Huang, J.-L.; Lieber, C. M. *Phys. Rev. Lett.* **1999**, *82*, 1225.
(39) Everson, M. P.; Jacklevic, R. C.; Shen, W. *J. Vac. Sci. Technol., A* **1990**, *8*, 3662.
(40) Hornbaker, D. J.; Kahng, S.-J.; Misra, S.; Smith, B. W.; Johnson, A. T.; Mele, E. J.; Luzzi, D. E.; Yazdani, A. *Science* **2002**, *828*, 295.
(41) Miyamoto, Y.; Saito, S.; Tomànek, D. *Phys. Rev. B* **2001**, *65*, 041402 (R).

NL070072P